Research Repository UCD

Title	A simple method for particle shape generation with spherical harmonics
Authors(s)	Wei, Deheng, Wang, Jianfeng, Zhao, Budi
Publication date	2018-05-01
Publication information	Wei, Deheng, Jianfeng Wang, and Budi Zhao. “A Simple Method for Particle Shape Generation with Spherical Harmonics.” Elsevier, May 1, 2018. https://doi.org/10.1016/j.powtec.2018.02.006.
Publisher	Elsevier
Item record/more information	http://hdl.handle.net/10197/12653
Publisher's statement	This is the author’s version of a work that was accepted for publication in Powder Technology. Changes resulting from the publishing process, such as peer review, editing, corrections, structural formatting, and other quality control mechanisms may not be reflected in this document. Changes may have been made to this work since it was submitted for publication. A definitive version was subsequently published in Powder Technology (330, (2018)) https://doi.org/10.1016/j.powtec.2018.02.006
Publisher's version (DOI)	10.1016/j.powtec.2018.02.006

Downloaded 2026-05-01 23:34:10

The UCD community has made this article openly available. Please share how this access benefits you. Your story matters! (@ucd_oa)

© Some rights reserved. For more information

A Simple Method for Particle Shape Generation with Spherical Harmonics

Deheng Wei[1], Jianfeng Wang[1] and Budi Zhao[1]

[1]Department of Architecture and Civil Engineering,
City University of Hong Kong, Hong Kong

Corresponding Author

Budi Zhao
Department of Architecture and Civil Engineering
City University of Hong Kong, Hong Kong
Tel: (852) 34426492
E-mail: bdzhao2-c@my.cityu.edu.hk

Abstract

The increasing interest in particle shape influence on granular mechanics necessitates a fast and robust particle shape generation method. We describe a new approach based on rotation-invariant spherical harmonic (SH) analysis. The core of this method is to construct morphology features at various length scales and superimpose them together to form the overall morphology. This method uses four rotation-invariant SH factors to construct SH coefficient matrices. We quantify particle shape at form, roundness, and compactness to establish the linkage between SH factors and traditional shape parameters. It is found that SH factors effectively control particle features at different scales. This method has a great potential to facilitate the research on granular mechanics considering particle shape effects.

Keywords

Compactness; form; particle morphology; particle generation; roundness; spherical harmonics.

1. Introduction

Particle morphology influences both mechanical and flow behavior of granular materials. For example, angular sands tend to have high shear strength (Cho et al., 2006, Ashmawy et al., 2003), stress concentration at contacts (Zhao et al, 2015; Wang and Coop, 2016), and resistance to flow and liquefaction (Cleary and Sawey, 2002, Antony and Kuhn, 2004). Also, particle morphology influences particle interactions with fluid and air, e.g., drag coefficient and mineral floatability (e.g., Haider and Levenspiel, 1989; Xia, 2017). Therefore, particle shape is an important parameter to predict and control the engineering properties of granular materials.

Recent years have witnessed a growing interest in representing particle shapes with mathematical methods. Optical microscopy, laser beam systems, digital holography and X-ray computed tomography have been used to obtain the morphology of particles (e.g., Altuhafi et al., 2012; Wu et al., 2016; Zhao and Wang, 2016). Real particle shapes can be effectively characterized and reconstructed at two-dimensional (2D) with Fourier analysis (e.g., Bowman et al., 2001) and at three-dimensional (3D) with spherical harmonic (SH) analysis (e.g., Garboczi, 2002; Zhou et al., 2015; Zhou and Wang, 2016; Zhou et al., 2017; Garboczi and Bullard, 2017). Meanwhile,

mathematical methods have shown great potential for particle shape generation. For example, Mollon and Zhao (2012) proposed an inverse operation to generate 2D particle shapes with given Fourier descriptors. They later extended the method to the 3D case based on 2D contours (Mollon and Zhao, 2013) and discrete random field (Mollon and Zhao, 2014). However, it remains a challenge to perform an inverse operation using SH analysis, i.e., to construct SH coefficient matrices for a particle with specified features.

In this study, we propose a simple method to generate 3D particle shapes with prescribed shape features using SH analysis. There are five sections in the following part of this paper. Section 2 briefly introduces the research background, including particle shape quantification method (Zhao and Wang, 2016) and rotation-invariant SH analysis (Zhao et al., 2017). Section 3 discusses the method to construct SH matrices with given SH factors. Section 4 shows the examples of generated particles and their shape quantification results. Section 5 discusses the advantage and disadvantage of the current method and provides a summary of this study.

2. Particle shape quantification and rotation-invariant SH analysis

2.1 Particle shape quantification

Particle shape is complicated to quantify due to its multi-scale nature. This study follows the particle shape quantification method proposed by Zhao and Wang (2016). Six shape parameters are calculated to quantify form, roundness, and compactness, as follows:

Form (*EI*, *FI*, and *AR*) As shown in Fig. 1(a), a 3D particle has three principal dimensions, $p_1 \geq p_2 \geq p_3$, determined by the principal component analysis (PCA). For 3D particles, particle form refers to two aspect ratios, namely elongation index ($EI=p_2/p_1$) and flatness index ($FI=p_3/p_2$). Their mean value is referred to as the characteristic aspect ratio (AR).

Roundness (R_M) Surface simplification is used to eliminate the influence of finer shape features (e.g., roughness) on particle roundness index. Particle roundness is quantified with the local curvature distribution at a particle surface with 1280 triangular elements. Zhao and Wang (2016) showed that surface roughness is effectively removed and particle corners are well identified with this level of surface simplification. Fig. 1(b) shows the distribution of mean curvature at particle corners.

Particle corners have larger curvature values than that of the particle's maximum inscribed sphere. Then, mean-curvature roundness index (R_M) is evaluated at the corners by the area-weighted average local mean curvature.

Compactness (S and C_X) Sphericity (S) describes how a particle is close to a sphere: $S = \frac{\sqrt[3]{36\pi V^2}}{SA}$, where V is particle volume, and SA is particle surface area. It compares the surface area of a particle and its volume-equivalent sphere (Fig. 1c). Convexity reflects how closely a particle represents a convex hull. This parameter is defined as $C_X = \frac{V}{V_{CH}}$, where V is particle volume and V_{CH} is the volume of its convex hull. Fig. 1(d) illustrates convex hull in two-dimension.

2.2 Rotation-invariant SH analysis

Spherical harmonics are a complete set of orthogonal functions defined on the surface of a sphere. This method originally used a radial representation, which is restricted to star-shaped surfaces. Brechbűhler et al. (1994) solved this limitation by introducing surface parameterization. Surface parameterization decomposes a 3D particle surface onto three orthogonal directions. It also enables establishing a linkage between SH coefficients and classical shape parameters (Zhao et al. 2017).

2.2.1 Surface parameterization

Surface parameterization creates a continuous and uniform mapping from particle surface to a unit sphere. Spherical parameterization results in a bijective mapping between each point on a surface and a pair of spherical coordinates:

$$\mathbf{v}(\theta,\ \phi) = \left(x(\theta,\ \phi),\ y(\theta,\ \phi),\ z(\theta,\ \phi)\right)^T, \tag{1}$$

where $(x(\theta,\phi),y(\theta,\phi),z(\theta,\ \phi))^{\mathrm{T}}$ is the Cartesian coordinates of a vertex, while $\theta\in[0,\pi]$ and $\phi\in[0,2\pi]$ are the latitudinal and longitudinal coordinates, respectively.

2.2.2 Spherical harmonic expansion

The coordination of the vertices on a particle surface could be represented by spherical harmonic expansion as:

$$\begin{pmatrix} x(\theta,\phi) \\ y(\theta,\phi) \\ z(\theta,\phi) \end{pmatrix} = \begin{pmatrix} \sum_{l=0}^{l_{\max}} \sum_{m=-l}^{l} c_{x,l}^{m} Y_l^m(\theta,\phi) \\ \sum_{l=0}^{l_{\max}} \sum_{m=-l}^{l} c_{y,l}^{m} Y_l^m(\theta,\phi) \\ \sum_{l=0}^{l_{\max}} \sum_{m=-l}^{l} c_{z,l}^{m} Y_l^m(\theta,\phi) \end{pmatrix}, \quad (2)$$

where Y_l^m and $(c_{x,l}^m, c_{y,l}^m, c_{z,l}^m)$ are the spherical harmonic and coefficients of degree l and order m, respectively. The definition of Y_l^m follows Press et al. (1992). $l_{\max}$ is the maximum SH degree used to reconstruct a particle surface.

SH analysis decomposes particle shape features into different SH degrees. For example, the shape features at an SH degree of l are characterized by:

$$\begin{pmatrix} x_l(\theta,\phi) \\ y_l(\theta,\phi) \\ z_l(\theta,\phi) \end{pmatrix} = \begin{pmatrix} c_{x,l}^{-l} & c_{x,l}^{-l+1} & \mathrm{L} & c_{x,l}^{l} \\ c_{y,l}^{-l} & c_{y,l}^{-l+1} & \mathrm{L} & c_{y,l}^{l} \\ c_{z,l}^{-l} & c_{z,l}^{-l+1} & \mathrm{L} & c_{z,l}^{l} \end{pmatrix} \begin{pmatrix} Y_l^{-l}(\theta,\phi) \\ Y_l^{-l+1}(\theta,\phi) \\ \mathrm{M} \\ Y_l^{l}(\theta,\phi) \end{pmatrix} = \mathbf{C}_l \mathbf{Y}_l(\theta,\phi), \quad (3)$$

where $\mathbf{C}_l$ is a $3\times(2l+1)$-dimensional matrix including the SH coefficients of degree l. $\mathbf{C}_0$ only influences particle position, which is not considered in this study. For l greater than zero, $\mathbf{C}_l$ contributes to finer shape features with increasing l. Specifically, $\mathbf{C}_1$ determines an ellipsoid, which is referred to as the first-degree ellipsoid (FDE).

2.2.3 Rotation-invariant SH analysis

Our previous study has defined two kinds of rotation-invariant factors from SH coefficients, i.e., spherical descriptors and their principal components (Zhao et al., 2017). These factors are only influenced by particle shape, not by particle position and rotation. Spherical descriptors are defined as:

$$d_l = \left\|\mathbf{C}_l\right\|_F = \sqrt{\sum_{i\in(\mathrm{x,y,z})} \sum_{m=-l}^{l} \left\|c_{i,l}^m\right\|^2} = \sqrt{\sum_{i\in(\mathrm{x,y,z})} \sum_{m=-l}^{l} c_{i,l}^m c_{i,l}^{m*}}, \quad (4)$$

where $\left\|\mathrm{g}\right\|_F$ is the Frobenius norm and * denotes the conjugate transpose. Parseval's theorem indicates that spherical descriptors are correlated with the mean squared distance (MSD) from particle surface to the origin: $\sum_{l}^{l_{\max}} d_l^2 = 4\pi \cdot \mathrm{MSD}$.

Spherical descriptors tend to decrease linearly with increasing SH degree in a

log-log scale. Fig. 2(a) shows the results obtained from 80 Leighton Buzzard sand (LBS) particles (Zhao et al., 2017). The spherical descriptors are normalized by d_1 to eliminate the influence of particle size. The average values of spherical descriptors tend to follow power-law equations:

$$\begin{cases} d_l = d_2 \cdot \left(\dfrac{2}{l}\right)^{\alpha} \quad for \quad l \in [2,8] \\ d_l = d_9 \cdot \left(\dfrac{9}{l}\right)^{\beta} \quad for \quad l \in [9,15] \end{cases} . \tag{5}$$

The fitted values of α and β are 1.387 and 1.426, respectively. Zhao et al. (2017) showed that major shape features (e.g., form, roundness and compactness) are well characterized with SH degrees up to eight. Therefore, we define tow sections in Eq. (5) to control different shape scales (i.e., roundness and roughness), although a single function could also fit well the descriptors. This correlation holds for any 40 randomly chosen particles with α and β in [1.320, 1.448] and [1.190, 1.672]. Zhao et al. (2017) show that similar correlations exist for LBS fragments that are more irregular than LBS particles. It is anticipated that these correlations also exist for other kinds of particles with different values of α and β. Then, the particles are aligned by rotating all the particles according to FDE, making p_1, p_2 and p_3 corresponding to x-, y- and z-axes, respectively. Therefore, the spherical descriptors are decomposed as $d_{i,l} = \sqrt{\sum_{m=-l}^{l} c_{i,l}^{m} c_{i,l}^{m*}}$ for i in (x, y, z). Fig. 2(b) shows the mean values of $d_{i,l}$ for 80 LBS particles, which are almost identical for l>1.

Previously, we defined two rotation-invariant SH factors, i.e., AR_{FDE} and d_{2-8}/d_1 (Zhao et al., 2017). AR_{FDE} is the characteristic aspect ratio for the first-degree ellipsoid (FDE). This factor has the dominant influence on particle form, i.e., aspect ratios. $d_{2-8}/d_1 = \sum_{l=2}^{8} d_l / d_1$ compares the MSDs of SH degrees between 2 and 8 to that of SH degree 1. This factor has a great influence on particle roundness. In this study, finer-scale features are also considered by including another SH factor, d_{9-15}/d_1, which is calculated as $d_{9-15}/d_1 = \sum_{l=9}^{15} d_l / d_1$.

3. SH coefficient matrices construction method

We propose a simple method to construct SH coefficient matrices using four SH factors, namely, the two aspect ratios of FDE (i.e., AR_{FDE} and EI_{FDE}), d_{2-8}/d_1, and d_{9-15}/d_1. SH coefficient matrices are constructed in two steps. First, an FDE with a major principal dimension of unit length and specified aspect ratios is generated. Second, the coefficient matrices of SH degrees between 2 and 8 (i.e., $\mathbf{C}_2-\mathbf{C}_8$) and those between 9 and 15 (i.e., $\mathbf{C}_9-\mathbf{C}_{15}$) are constructed from the value of d_{2-8}/d_1 and d_{9-15}/d_1, respectively.

Step-1: First-degree ellipsoid (FDE) with specified EI_{FDE} and FI_{FDE} values ($\mathbf{C}_1$)

The shape of an FDE is uniquely determined by its *EI* and *FI* values and a unit major principal dimension. Its principal dimensions ($p_1 \geq p_2 \geq p_3$) are $p_1=1$, $p_2=EI$ and $p_3=EI\times FI$. Then, FDE's coefficient matrix, $\mathbf{C}_1$, is constructed as $-\sqrt{\frac{\pi}{6}}\begin{pmatrix} -1 & 0 & 1 \\ EI\times i & 0 & EI\times i \\ 0 & \sqrt{2}EI\times FI & 0 \end{pmatrix}$, where i is the imaginary unit. The generated FDEs have three principal dimensions, p_1, p_2, and p_3, corresponding to *x*-, *y*- and *z*-axes, respectively.

Step-2: Coefficients of SH degrees between 2 and 15 ($\mathbf{C}_2-\mathbf{C}_8$ and $\mathbf{C}_9-\mathbf{C}_{15}$) with specified values of d_{2-8}/d_1 and d_{9-15}/d_1

The values of d_l for l between 2 and 8 are determined from the specified value of d_{2-8}/d_1 according to Eq. (5) and the value of d_1 defined in Step-1. Then, we assume the spherical descriptors have the equivalent decompositions at three coordination axes, i.e., $d_{x,l}=d_{y,l}=d_{z,l}$. This assumption will balance the decompositions of MSD on three coordination axes. Therefore, the coefficients of $l>1$ have limited influence on particle form.

The SH coefficients of $\mathbf{C}_l$ are complex numbers that have to satisfy $c_n^{-m}=(-1)^m c_n^{m*}$ to make the coordinates of vertices to be real numbers. To satisfy this

requirement, the form of $\mathbf{C}_l$ is assumed as

$$\mathbf{C}_l = \begin{pmatrix} c_{x,l}^{-l} & \mathrm{L} & c_{x,l}^{0} & \mathrm{L} & c_{x,l}^{l} \\ c_{y,l}^{-l} & \mathrm{L} & c_{y,l}^{0} & \mathrm{L} & c_{y,l}^{l} \\ c_{z,l}^{-l} & \mathrm{L} & c_{z,l}^{0} & \mathrm{L} & c_{z,l}^{l} \end{pmatrix} = \begin{pmatrix} k_x(\alpha_{2l} - \alpha_{2l+1} i) & \mathrm{L} & k_x \alpha_1 & \mathrm{L} & k_x(\alpha_{2l} + \alpha_{2l+1} i) \\ k_y(\beta_{2l} - \beta_{2l+1} i) & \mathrm{L} & k_y \beta_1 & \mathrm{L} & k_y(\beta_{2l} + \beta_{2l+1} i) \\ k_z(\varepsilon_{2l} - \varepsilon_{2l+1} i) & \mathrm{L} & k_z \varepsilon_1 & \mathrm{L} & k_z(\varepsilon_{2l} + \varepsilon_{2l+1} i) \end{pmatrix}, \quad (6)$$

where $(\alpha_i, \beta_i, \varepsilon_i)$ for $i \in [1, 2l+1]$ are real numbers between 0 and 1, which are randomly generated with a uniform distribution. k_x, k_y and k_z are three normalizing factors. The values of k_x, k_y and k_z are determined from the values of $d_{x,l}$, $d_{y,l}$ and $d_{z,l}$, e.g., $k_x = \sqrt{d_{x,l}^2 / (\alpha_1^2 + 2\sum_{i=2}^{2l+1} \alpha_i^2)}$. This procedure is repeated for SH degrees between 2 and 8. So far, the coefficient matrices for SH degrees between 2 and 8 are constructed from one specified value of d_{2-8} / d_1. Similarly, the coefficient matrices of SH degrees between 9 and 15 are determined from d_{9-15} / d_1.

4. Particle shape generation results

In this section, SH coefficient matrices are constructed with a series of SH factors. Then, 3D particle shapes were reconstructed from SH matrices through Eq. 2. The SPHARM-MAT Toolbox is used to perform SH expansion and represent particle shapes with triangular surface meshes for visualization and shape quantification (available at http://www.iu.edu/~shenlab/software.html).

We first randomly generated three particles from the spherical descriptors of a real LBS particle for SH degrees between 2 and 15. The FDEs for these particles are all unit diameter spheres. Fig. 3 shows the expansions of particles with one or more degrees of SHs superimposing on their FDEs. It shows that higher SH degree describes finer-scale particle features. For example, SH degrees 2 and 4 describe particle roundness, while SH degree 10 describes particle roughness. The overall particle features are well characterized with SH degrees up to 8. The three particles also reflect the randomness of this particle generation method. They have a similar level of irregularity with the original LBS particle but distinct shapes.

A series of AR_{FDE} (EI_{FDE}) and $d_{2\text{-}8}/d_1$ are used to generate particles with different

level of irregularity (Fig. 4). AR_{FDE} (EI_{FDE}) has a dominant influence on particle form. Particles with large AR_{FDE} (EI_{FDE}) values have almost identical principal dimensions. As AR_{FDE} (EI_{FDE}) reduces, particles become more elongated. By increasing $d_{2\text{-}8}/d_1$, particles' angularity gradually increases from well rounded to very angular. An example of well-rounded and angular particle could be pebble and rock ballast, respectively. Fig.5 shows three particles with different values of $d_{9\text{-}15}/d_1$, while AR_{FDE} (EI_{FDE}) and $d_{2\text{-}8}/d_1$ are set as 0.9 (0.9) and zero. It shows that $d_{9\text{-}15}/d_1$ changes particle roughness without affecting the overall shape.

The influence of SH factors on generated particle shapes are quantitatively investigated using alternate combinations of AR_{FDE} (EI_{FDE}) = {0.5 (0.3); 0.6 (0.5); 0.7 (0.6); 0.8 (0.7); 0.9 (0.9)} and $d_{2\text{-}8}/d_1$ = {0.0; 0.1; 0.2; 0.3; 0.4; 0.5; 0.6} while keeping $d_{9\text{-}15}/d_1$ equal to zero. For each combination of AR_{FDE} (EI_{FDE}) and $d_{2\text{-}8}/d_1$, we randomly generated two hundred particles. Their triangular surface meshes are then quantified at form, roundness and compactness. Fig.6 plots the average values of the shape parameters of two hundred particles in each group. It shows that particle form (AR) and roundness (R_M) are mainly influenced by AR_{FDE} (EI_{FDE}) and $d_{2\text{-}8}/d_1$, respectively. Compactness (S and C_X) is influenced by both AR_{FDE} (EI_{FDE}) and $d_{2\text{-}8}/d_1$. Similarly, two hundred particles are randomly generated for alternate combinations of AR_{FDE} (EI_{FDE}) = {0.5 (0.3); 0.6 (0.5); 0.7 (0.6); 0.8 (0.7); 0.9 (0.9)} and $d_{9\text{-}15}/d_1$ = {0.0; 0.01; 0.02; 0.03; 0.04; 0.05; 0.06} while keeping $d_{2\text{-}8}/d_1$ equal to zero. Fig.7 shows that $d_{9\text{-}15}/d_1$ has a much smaller influence on particle shape parameters than $d_{2\text{-}8}/d_1$. Only when AR_{FDE} (EI_{FDE}) is large, particle roundness is slightly influenced by $d_{9\text{-}15}/d_1$.

The two hundred particles in each group generated with the same SH factors have similar level of irregularity but different shapes. To illustrate this, we picked seven groups of particles corresponding to the red points in Fig.6. Fig.8 plots the distributions of their shape parameters. The distributions with enough data points are fitted with Gaussian function with an offset. The two hundred particles with $d_{2\text{-}8}/d_1$ equal to zero have the same shape parameters. They are identical ellipsoids with the same AR_{FDE} (EI_{FDE}) and a unit major principal dimension. The randomness of generated shapes is only introduced by $d_{2\text{-}8}/d_1$ and $d_{9\text{-}15}/d_1$. The variance of all shape parameters increases with increasing $d_{2\text{-}8}/d_1$.

5. Discussion and summary

We proposed a simple method to randomly generate 3D particle shapes with a

specified level of irregularity. The SH factors used to generate particle shapes are well correlated with the classical particle parameters. The method has a solid mathematical foundation, i.e., rotation-invariant SH analysis. Therefore, it has great efficiency in calculation and storage cost. For example, generating the SH coefficients (C_1-C_{15}) of one thousand particles only need 3.70 seconds with an Intel i5-4590 CPU (4 cores, 3.3 GHz). These coefficients can be stored in a MAT-file of 5.8 MB. In comparison, generating ten particles takes more than four hours with the discrete random field method proposed in Mollon and Zhao (2014) using the same computer. The MAT-file storing the shape matrix is about 100 MB. Also, the SH descriptors used for particle generation have a strong relationship with classical particle shape parameters. This relationship could serve as an input for generating particles with required shape parameters. The particles generated by this method tend to be smooth due to the nature of SH method. Therefore, it is costly to simulate sharp corners that are common in particle fragments and materials formed via crystallization. It is noticed that further study is needed to understand the influence of the empirical correlation in Eq. (5) on the generated particle shapes.

It remains a challenge to quantitatively correlate the micro- and macro-mechanical behaviour of granular assemblies with particle shape. The difficulties mainly arise from the multi-scale nature of particle shape. Also, real particles always have distinct shapes even though they have similar irregularity. For example, no two pebbles are exactly alike, although they are well rounded. The method proposed in this study has great potential for future numerical and experimental studies (e.g. discrete element method and 3D printer) on particle shape. The generated particle shapes have similar irregularity but remains different. This randomness of particle shapes could lead to the a certain level of randomness into the micro- and macro-mechanical behaviour of granular assemblies. However, they should have similar micro- and macro-mechanical behaviours if the behaviours are well correlated with shape irregularity. In addition, a single particle shape could be used to elliminate this randomness.

6. Acknowledgement

The study was supported by Research Grant No. 51379180 from the National Science Foundation of China General Research Fund No. CityU 11272916 from the Research Grant Council of the Hong Kong SAR and the open-research grant No. SLDRCE15-04 from State Key Laboratory of Civil Engineering Disaster Prevention

of Tongji University.

Notation list

AR	aspect ratio index
AR_{FDE}	aspect ration index of first-degree ellipsoid
$\mathbf{C}_l$	spherical harmonic coefficients matrix of SH degree l
$c_{x,l}^m, c_{y,l}^m, c_{z,l}^m$	spherical harmonic coefficient for degree l and order m corresponding to x, y and z coordinates
C_{X}	convexity
d_l	spherical descriptor of SH degree l
$d_{x,l}$, $d_{y,l}$ and $d_{z,l}$	three components of d_l corresponding to x, y and z coordinates
$e_{l,1} \geq e_{l,2} \geq e_{l,3}$	three eigenvalues of $\mathbf{C}_l\mathbf{C}_l^*$
EI_{FDE}	elongation index of first-degree ellipsoid
EI	elongation index
FDE	first-degree ellipsoid
FI	flatness index
$p_1 \geq p_2 \geq p_3$	three principal dimensions of FDE
R_{M}	roundness index based on local mean curvature
S	sphericity
SA	surface area
V	volume
V_{CH}	volume of convex hull
$\mathbf{v}_{\theta,\phi}$	Cartesian coordinates vector
Y_l^m	spherical harmonic function for degree l and order m

7. References

Altuhafi F, O'sullivan C, Cavarretta I. Analysis of an image-based method to quantify the size and shape of sand particles. Journal of Geotechnical and Geoenvironmental Engineering, 2012, 139(8):1290-1307.

Antony S J, Kuhn M R. Influence of particle shape on granular contact signatures and shear strength: new insights from simulations. International Journal of Solids and Structures, 2004, 41(21): 5863-5870.

Ashmawy A K, Hoang V V, Sukumaran B. Evaluating the influence of particle shape on liquefaction behavior using discrete element modeling. Proc. Of thirteenth international offshore and polar Engineering conference, Hawaii, USA, 2003.

Bowman E T, Soga K, Drummond W. Particle shape characterisation using Fourier descriptor analysis. Géotechnique, 2000, 51(6): 545-554.

Brechbühler C, Gerig G, O. Kübler. Parametrization of Closed Surfaces for 3-D Shape Description. Computer Vision and Image Understanding, 1995, 61(2): 154-170.

Cho G C, Dodds J, Santamarina J C. Particle shape effects on packing density, stiffness, and strength: natural and crushed sands. Journal of Geotechnical & Geoenvironmental Engineering, 2006, 133(11): 591-602.

Cleary P W, Sawley M L. DEM modelling of industrial granular flows: 3D case studies and the effect of particle shape on hopper discharge. Applied Mathematical Modelling, 2002, 26(2): 89-111.

Garboczi E J. Three-dimensional mathematical analysis of particle shape using X-ray tomography and spherical harmonics: application to aggregates used in concrete. Cement and Concrete Research, 2002, 32(10): 1621-1638.

Garboczi E J, Bullard J W. 3D analytical mathematical models of random star-shape particles via a combination of X-ray computed microtomography and spherical harmonic analysis. Advanced Powder Technology, 2017, 28(2): 325-339.

Haider A, Levenspiel O. Drag coefficient and terminal velocity of spherical and nonspherical particles. Powder Technology, 1989, 58(1): 63-70.

Mollon G, Zhao J. Fourier–Voronoi-based generation of realistic samples for discrete modelling of granular materials. Granular Matter, 2012, 14(5): 621-638.

Mollon G, Zhao J. Generating realistic 3D sand particles using Fourier descriptors. Granular Matter, 2013, 15(1): 95-108.

Mollon G, Zhao J. 3D generation of realistic granular samples based on random fields theory and Fourier shape descriptors. Computer Methods in Applied Mechanics & Engineering, 2014, 279(279): 46-65.

Press W H, Teukolsky S A, Vetterling W T, Flannery B P. Numerical recipes in C: the art of scientific computing, 2nd edn. Cambridge University Press, Cambridge, UK, 1992.

Wang W, Coop M R. An investigation of breakage behaviour of single sand particles using a high-speed microscope camera. Géotechnique, 2016, 66(12): 984-998.

Wu Y, Wu X, Yao L, Brunel M, Coëtmellec S, Lebrun D, Gréhan G, Cen K. 3D

boundary line measurement of irregular particle with digital holography. Powder Technology, 2016, 295: 96-103.

Xia W. Role of particle shape in the floatability of mineral particle: an overview of recent advances. Powder Technology, 2017, 317: 104-116.

Zhao B, Wei D, Wang J. Particle shape quantification using rotation-invariant spherical harmonic analysis. Géotechnique Letters, 2017, 7(2).

Zhao B, Wang J. 3D quantitative shape analysis on form, roundness, and compactness with μCT. Powder Technology, 2016, 291: 262-275.

Zhao B, Wang J, Coop M R, Viggiani G, Jiang M. An investigation of single sand particle fracture using X-ray micro-tomography. Géotechnique, 2015, 65(8): 625-641.

Zhou B, Wang J, Zhao B. Micromorphology characterization and reconstruction of sand particles using micro X-ray tomography and spherical harmonics. Engineering Geology, 2015, 184(14): 126-137.

Zhou B, Wang J. Generation of a realistic 3D sand assembly using X-ray micro-computed tomography and spherical harmonic-based principal component analysis. International Journal for Numerical and Analytical Methods in Geomechanics, 2017, 41(1): 93-109.

Zhou B, Wang J, Wang H. Three-dimensional sphericity, roundness and fractal dimension of sand particles. Géotechnique, 2017.

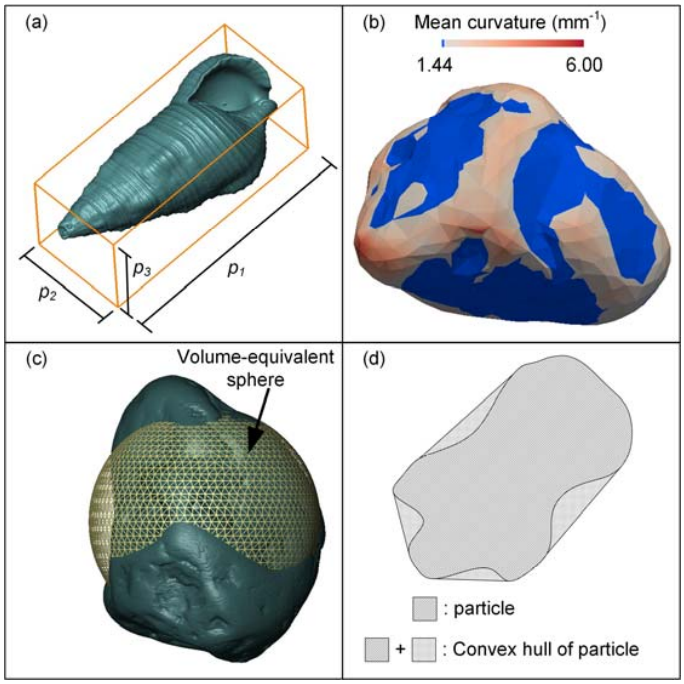

Fig. 1 Illustration of shape parameters: (a) aspect ratios ($EI=p_2/p_1$, $FI=p_3/p_2$, $AR=(EI+FI)/2$); (b) mean-curvature roundness index (R_M); (c) sphericity (S); (d) convexity (C_X).

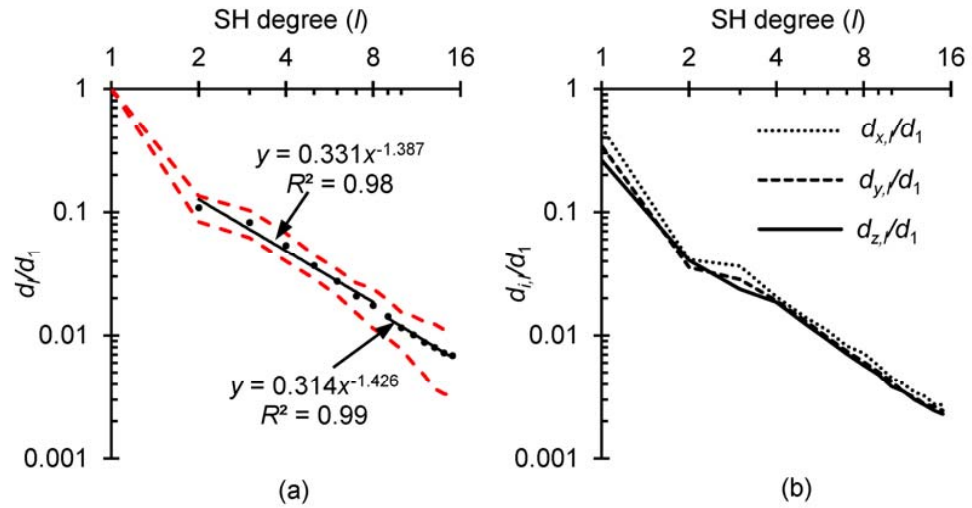

Fig. 2 Spherical descriptors of 80 LBS particles: (a) spherical descriptors at each SH degree (solid lines: mean value; dashed lines: mean value ± standard deviation) and (b) mean values of spherical descriptors decompositions at x, y and z axes

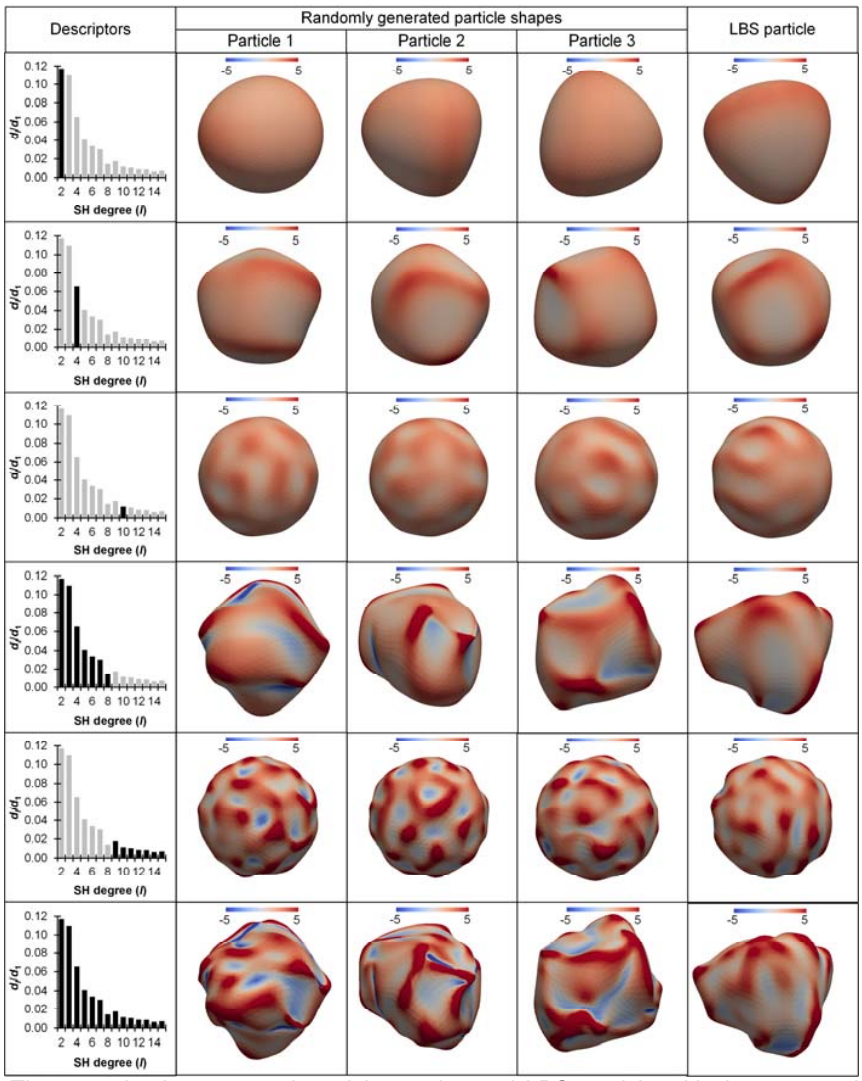

Fig. 3 Three randomly generated particles and a real LBS particle with the same spherical descriptors (d_2-d_{15}) superimposed on a unit diameter sphere, different SH degrees are used to reconstruct the surfaces (colour of surfaces indicates the distribution of mean curvature, L^{-1})

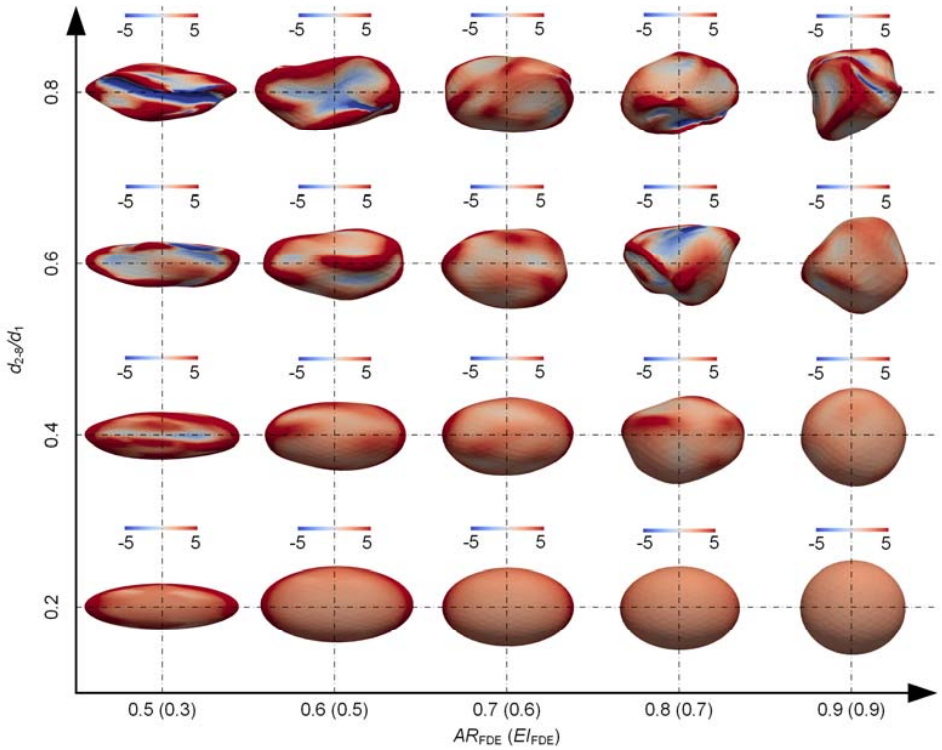

Fig. 4 Influence of AR_{FDE} (EI_{FDE}) and $d_{2\text{-}8}/d_1$ on the shapes of generated particles (colour of surfaces indicates the distribution of mean curvature, L^{-1})

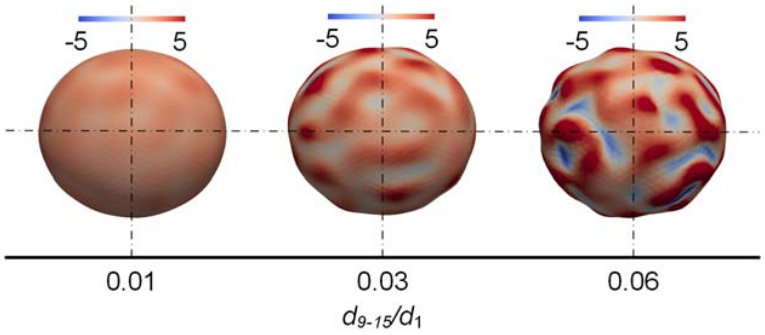

Fig. 5 Influence of $d_{9\text{-}15}/d_1$ on the shapes of generated particles (colour of surfaces indicates the distribution of mean curvature, L^{-1})

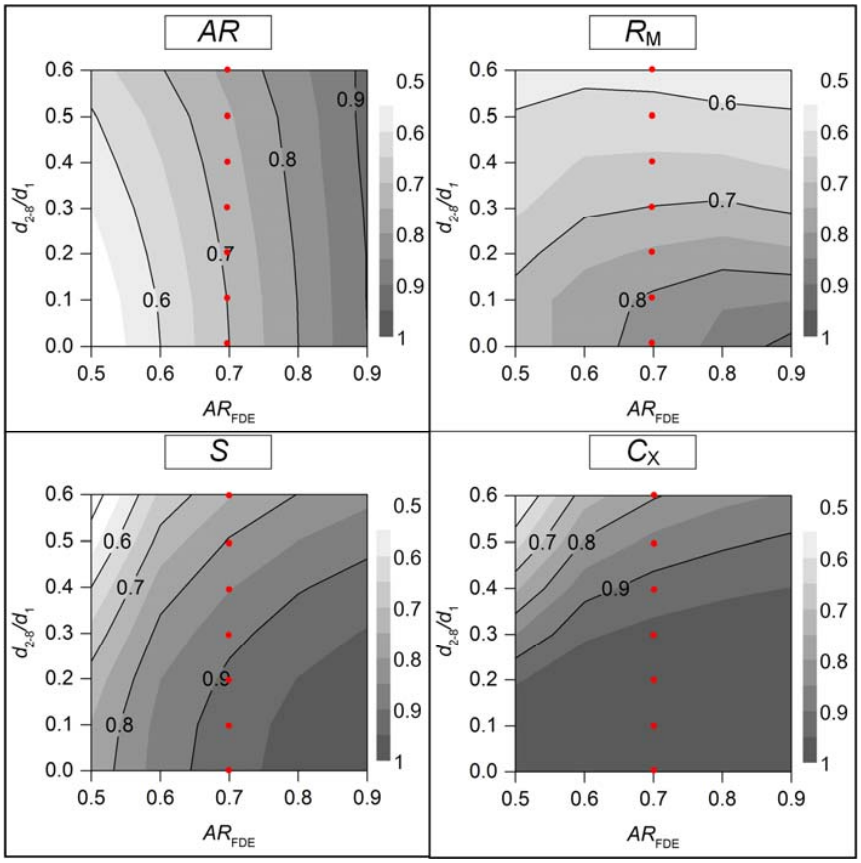

Fig. 6 Mean values of shape parameters (*AR*, R_M, *S* and C_X) of 200 randomly generated particles in each combination of AR_{FDE} (EI_{FDE}) = {0.5 (0.3); 0.6 (0.5); 0.7 (0.6); 0.8 (0.7); 0.9 (0.9)} and $d_{2\text{-}8}/d_1$ = {0.0; 0.1; 0.2; 0.3; 0.4; 0.5; 0.6}, while $d_{9\text{-}15}/d_1$ = {0.0}

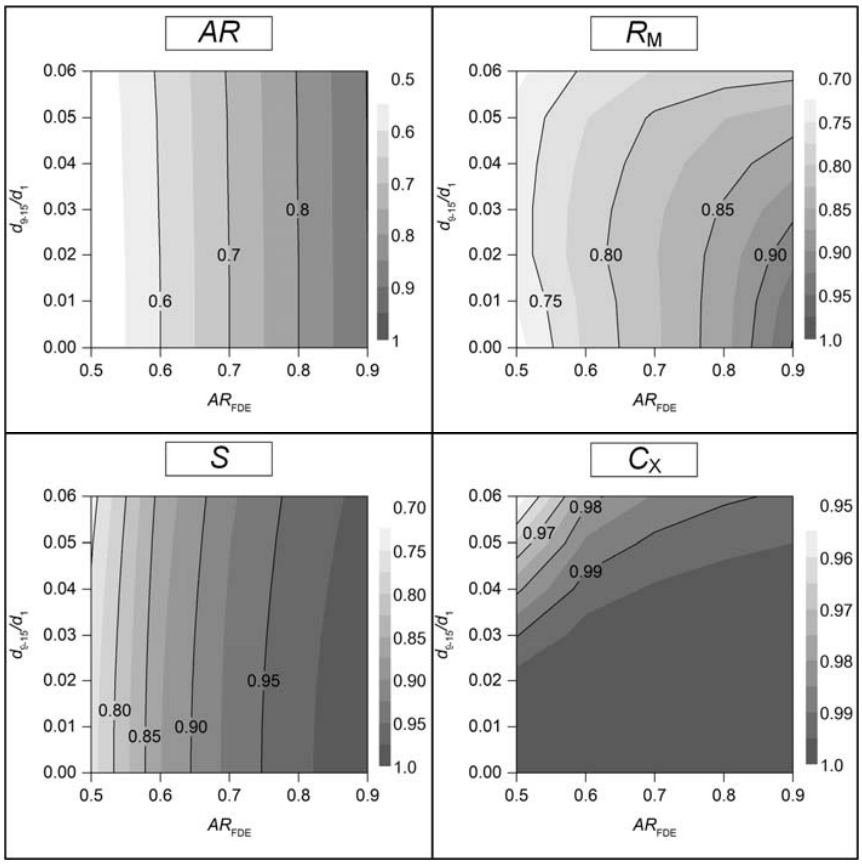

Fig. 7 Mean values of shape parameters (*AR*, R_M, *S* and C_X) of 200 randomly generated particles in each combination of AR_{FDE} (EI_{FDE}) = {0.5 (0.3); 0.6 (0.5); 0.7 (0.6); 0.8 (0.7); 0.9 (0.9)} and $d_{9\text{-}15}/d_1$ = {0.0; 0.01; 0.02; 0.03; 0.04; 0.05; 0.06}, while $d_{2\text{-}8}/d_1$ = {0.0}

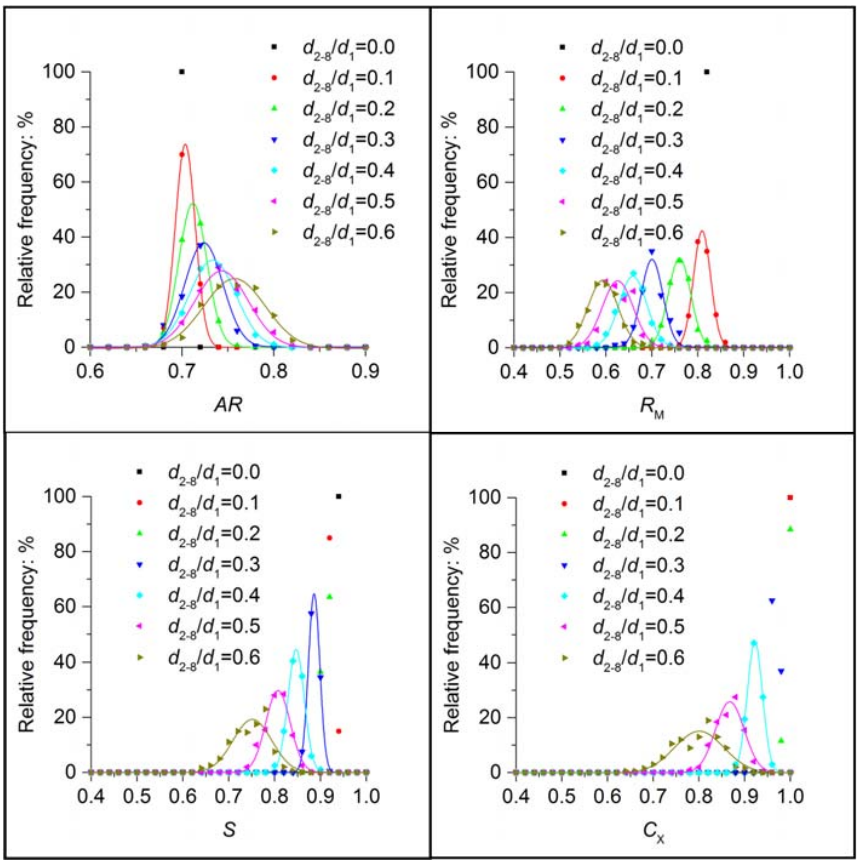

Fig. 8 Distributions of shape parameters (*AR*, R_M, *S* and C_X) of 200 randomly generated particles in combinations of AR_{FDE} (EI_{FDE}) = {0.7 (0.6)}, $d_{2\text{-}8}/d_1$ = {0.0; 0.1; 0.2; 0.3; 0.4; 0.5; 0.6} and $d_{9\text{-}15}/d_1$ = {0.0} (distributions with enough data points are fitted with Gaussian function) (corresponding to the red points in Fig.6)